Antiferromagnetism in $CoCl_2 \cdot 2H_2O$. I. Magnetic Structure*

ALBERT NARATH
Sandia Laboratory, Albuquerque, New Mexico
(Received 21 May 1964)

The magnetic structure of $CoCl_2 \cdot 2H_2O$ has been investigated by means of single-crystal magnetic susceptibility and proton nuclear magnetic resonance (NMR) measurements. A transition to a two-sublattice antiferromagnetic structure with large uniaxial anisotropy occurs below 17.5°K. The measured paramagnetic susceptibilities yield $g_{II}=7.3$, $g_{\perp}=2.9$, and temperature-independent contributions $N\alpha_{II}=0.0033$, $N\alpha_{\perp}=0.0129$ emu/mole. The Curie-Weiss constant is very small, $\theta=1\pm1$°K, giving evidence for ferromagnetic and antiferromagnetic exchange energies of equal magnitude. The zero-field proton NMR consists of a single spin-spin doublet with center frequency $\nu_0(^1H)=17.944\pm0.003$ Mc/sec at $T\leq4$°K. From rotation studies of the proton NMR in weak external magnetic fields an ordered magnetic structure ($Pc2/m$) is inferred in which ferromagnetic $-CoCl_2-$ chains, parallel to the c axis, are coupled antiferromagnetically to adjacent chains. The b axis is the preferred direction of magnetization.

I. INTRODUCTION

THE extensive investigations of the magnetic properties of antiferromagnetic $CuCl_2 \cdot 2H_2O$ at Leiden[1] have stimulated much interest in the properties of other hydrated iron-group halides. Unfortunately, the structures of these halides in their stable hydration states (e.g., $MnCl_2 \cdot 4H_2O$, $FeCl_2 \cdot 4H_2O$, $CoCl_2 \cdot 6H_2O$, $NiCl_2 \cdot 6H_2O$, etc.) are fairly complex in contrast to the simple orthorhombic ($Pbmn$) crystal structure of $CuCl_2 \cdot 2H_2O$.[2] For this reason unambiguous interpretations of the experimental observations have often been impossible. By crystallizing the appropriate halides from aqueous solution at slightly elevated temperatures, however, one can obtain a series of crystalline compounds of the type $MX_2 \cdot 2H_2O$, where $M \equiv$ Mn, Fe, Co, Ni, and $X \equiv$ Cl, Br. These compounds are closely related structurally[3,4] to $CuCl_2 \cdot 2H_2O$. We have examined the powder susceptibilities of these compounds for evidence of magnetic ordering and have found that the Fe, Co, and Ni salts undergo transitions to magnetically ordered states at temperatures above 15°K. (The corresponding manganese salts have anomalously low-transition temperatures, ~2°K, similar to $MnCl_2$ and $MnCl_2 \cdot 4H_2O$.[5]) Because of the large exchange energies which can be inferred from these measurements (in contrast to the situation in most other hydrated iron-group salts), and because of the simplicity of the corresponding crystal structures, a study of the magnetic properties of these compounds promises to be quite rewarding.

The present paper is concerned with an investigation of the magnetic structure of $CoCl_2 \cdot 2H_2O$ by single-crystal magnetic susceptibility and proton nuclear magnetic resonance (NMR) measurements. The crystal structure of $CoCl_2 \cdot 2H_2O$ is reviewed in Sec. II; the details of our experimental techniques are given in Sec. III. In Sec. IV, the results of our magnetic susceptibility measurements are given. Section V is concerned with our proton NMR measurements and the magnetic structure which can be inferred from them. In Sec. VI, we compare our results with previous measurements on $CoCl_2$ and $CoCl_2 \cdot 6H_2O$.

TABLE I. Room-temperature lattice parameters and atomic coordinates of $CoCl_2 \cdot 2H_2O$.

$C2/m$: $a_0=7.256$ Å, $b_0=8.575$ Å, $c_0=3.554$ Å; $\beta=97°33'$			
Position	a	b	c
Co	0	0	0
Cl	0.2373	0	0.5582
O	0	0.2378	0
H	0.06	0.30	0.16

II. CRYSTAL STRUCTURE

The structure of $CoCl_2 \cdot 2H_2O$ was first deduced by Vainshtein[6] using electron diffraction techniques. Recently, Morosin and Graeber[3] refined the structure by x-ray diffraction techniques. The room-temperature lattice constants and atomic coordinates are given in Table I. The structure has monoclinic symmetry (space group $C2/m$) and is made up of polymeric $-CoCl_2-$ chains parallel to the c axis which are held together by relatively weak hydrogen bonds.

In Fig. 1, the nearly symmetric chlorine bridging in the $-CoCl_2-$ chains is compared with the highly asymmetric bridging found in $CuCl_2 \cdot 2H_2O$. The Co^{2+} ions are surrounded by a nearly perfect square planar arrangement of Cl^- ions in (010) planes; the nearest-neighbor octahedron is completed by the hydrate oxygens. The crystal-field symmetry at the cobalt sites is therefore nearly tetragonal; furthermore, the principal axis of the crystal field coincides with the twofold crystallographic symmetry axis (b axis). The analysis

* This work was supported by the U. S. Atomic Energy Commission. Reproduction in whole or in part is permitted for any purpose of the U. S. Government.

[1] C. J. Gorter, Rev. Mod. Phys. **25**, 332 (1953); this paper is a review of the important references.

[2] D. Harker, Z. Krist. **93**, 136 (1936).

[3] B. Morosin and E. J. Graeber, Acta Cryst. **16**, 1176 (1963).

[4] B. Morosin and E. J. Graeber (to be published).

[5] R. B. Murray, Phys. Rev. **100**, 1071 (1955); H. M. Gijsman, N. J. Poulis, and J. Van Den Handel, Physica **25**, 954 (1959).

[6] B. K. Vainshtein, Dokl. Akad. Nauk. SSSR **68**, 301 (1949).

of the magnetic properties of $CoCl_2 \cdot 2H_2O$ is further simplified by the fact that the two cobalt sites in the unit cell are related by the lattice centering and hence are equivalent.

The packing of the $-CoCl_2-$ chains is illustrated in Fig. 2. The slight monoclinic distortion of the structure is evidently caused by the hydrogen bonding. The bonding between the chains is quite weak as evidenced by the pronounced cleavage of $CoCl_2 \cdot 2H_2O$ crystals in any plane parallel to the c axis.

The dihydrated chlorides and bromides of Mn, Fe, and Co form an isomorphous series.[4] The corresponding nickel salts are very similar but differ slightly in the packing of the chains.[4]

III. EXPERIMENTAL PROCEDURES

The starting materials for sample preparation consisted of $CoCl_2 \cdot 6H_2O$ (commercial reagent grade, Ni low) and $CoCl_2$ obtained by chlorinating Co metal (Johnson Matthey). No measurable differences were observed in the properties of $CoCl_2 \cdot 2H_2O$ crystals prepared from the two different sources.

Single crystals of $CoCl_2 \cdot 2H_2O$ were prepared by slow evaporation at 70°C of a saturated aqueous solution whose temperature was kept constant within ± 0.05°C by a thermostated oil bath. The very high solubility of $CoCl_2 \cdot 2H_2O$ at 70°C necessitated great care in sealing the evaporation chambers in order to maintain slow, uniform evaporation rates. The crystals have a pronounced [001] preferred growth habit and usually exhibit well developed (110) type faces. We were able to obtain single crystals (free of macroscopic defects) as large as $1 \times 1 \times 5$ cm by the evaporation technique. Although the stable hydrate at room temperature is the hexahydrate, the dihydrated crystals are not very hygroscopic; a thin coating of oil was the only protection from atmospheric moisture which was needed. Single-crystal specimens used in the present study were oriented by x-ray diffraction techniques within an accuracy of 1°.

Magnetic susceptibility measurements were made by the mutual inductance method. The mutual inductor consisted of a multiturn primary wound coaxially on an astatic secondary winding. The coils were immersed in a pumped (1.2°K) liquid-helium bath, and were mounted on the outside of an unsilvered, vacuum-jacketed glass Dewar which contained the sample assembly. The sample was provided with a thin phenolic thermal radiation shield and made good thermal contact through several thin copper wires with the thermometer and heater (which were kept a few centimeters above the mutual inductor). The sample assembly could be pulled out of the coil and all measurements were based on differences in the observed mutual inductances with the sample in and out of one of the secondary windings. Inductance measurements were made with a Cryotronics Model ML155B mutual inductance bridge at a frequency of 155 cps. The apparatus was calibrated against the magnetic susceptibility of $Fe(NH_4)_2(SO_4)_2 \cdot 6H_2O$.[7]

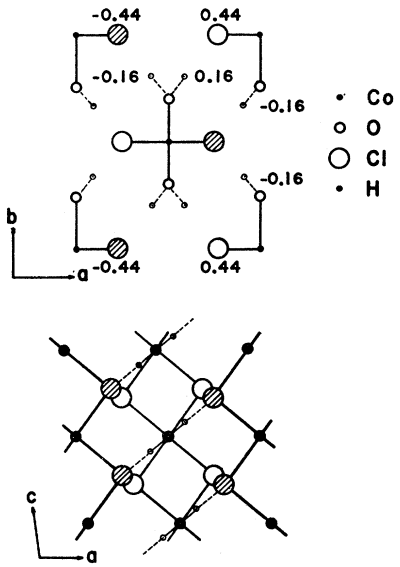

FIG. 2. Crystal structure of $CoCl_2 \cdot 2H_2O$. Top: Projection along the c axis. Bottom: Projection along the b axis.

The proton magnetic resonances were observed with the frequency swept FM marginal oscillator shown in Fig. 3, followed by a conventional synchronous detector operating at 400 cps. By using shunt coils outside the cryostat, the oscillator could be made to cover the range 10–60 Mc/sec with a single sample coil. This was made possible by the feedback arrangement employed in our design which permits oscillations to be sustained even when the tank L/C ratio is very small. At 4°K, the samples were immersed directly in liquid helium; higher temperatures were obtained in a vacuum-jacketed heat-leak chamber which was provided with a heater.

Temperature measurements above 25°K were made with a copper-constantan thermocouple; below 25°K, a calibrated germanium resistance thermometer was used.

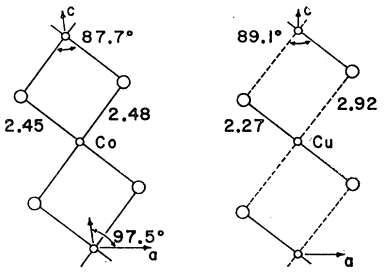

FIG. 1. Comparison of the polymeric $-MCl_2-$ chains in the crystal structures of $CoCl_2 \cdot 2H_2O$ and $CuCl_2 \cdot 2H_2O$.

IV. MAGNETIC SUSCEPTIBILITY

The magnetic susceptibilities of $CoCl_2 \cdot 2H_2O$ were measured along the a^*, b, and c axes, and the results

[7] G. A. Candela and R. E. Mundy, Rev. Sci. Instr. 32, 1056 (1961).

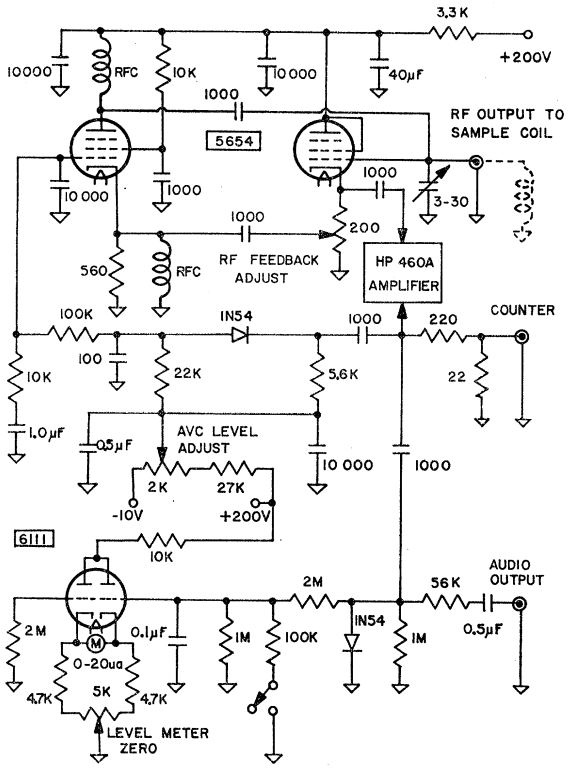

FIG. 3. Schematic of marginal oscillator. Frequency modulation is accomplished by vibrating capacitor or voltage-variable capacitor.

are summarized in Fig. 4. The experimental values confirm the uniaxial character of the magnetic anisotropy expected on the basis of the tetragonal symmetry of the Co^{2+} environment. The measurements show that $CoCl_2 \cdot 2H_2O$ becomes antiferromagnetically ordered below $\sim 17.5°K$, with sublattice magnetizations directed parallel to the b axis.

The theory of the g values and magnetic susceptibilities of Co^{2+} in magnetically dilute crystals has been given in detail by Abragam and Pryce,[8] and by Kambe *et al.*[9] The $(3d)^7$ configuration of Co^{2+} gives rise to two triplet states and a single state in the lowest ^4F ($L=3$, $S=\frac{3}{2}$) term in an octahedral crystal field. The ground orbital triplet splits into six Kramers doublets under the combined action of spin-orbit coupling and tetragonal distortion of the crystal field. In $CoCl_2 \cdot 2H_2O$ the tetragonal component is quite large and the separation of the two lowest doublets is probably several hundred wave numbers. Since our measurements were restricted to temperatures below 150°K, the magnetic susceptibilities should be characteristic of a twofold degenerate ground state which is separated by more than kT from higher lying states. Furthermore, an inspection of our χ_b^{-1} data in the paramagnetic range of $CoCl_2 \cdot 2H_2O$ indicates that exchange effects make a very small contribution to the observed paramagnetic susceptibilities. Consequently, the susceptibilities should follow the relation[10]

$$\chi_i = [N g_i^2 \mu_B^2 S(S+1)/3kT] + N\alpha_i, \qquad (1)$$

where χ_i is the ith principal component of the susceptibility tensor, g_i is the effective g value, μ_B is the Bohr magneton, $S=\frac{1}{2}$ is the effective spin of the ground-state doublet, and α_i is the temperature-independent contribution arising from high-frequency elements of the paramagnetic moment and from small diamagnetic effects. In the range 25–100°K our data follow Eq. (1) within our experimental error. The extrapolated intercepts of χ_i versus T^{-1} plots yield

$$N\alpha_{\parallel} \equiv N\alpha_b = 0.0033 \text{ emu/mole},$$
$$N\alpha_{\perp} \equiv N\alpha_c = 0.0129 \text{ emu/mole},$$

and the slopes

$$g_{\parallel} \equiv g_b = 7.3,$$
$$g_{\perp} \equiv g_c = 2.9.$$

The extrapolated temperature intercepts of $(\chi_i - N\alpha_i)^{-1}$ versus T in both cases occur at $T = 1 \pm 1°K$, which confirms that the Curie-Weiss constant θ is much smaller than the Néel temperature T_N, and hence justifies our use of Eq. (1). Our results for χ_{a^*} are less accurate than those for χ_b, χ_c because of the small size of the crystal used in the a^* measurements; however, within our experimental uncertainty the values obtained for α_{a^*} and g_{a^*} agree with the corresponding c-axis values.

A detailed analysis of our measured susceptibilities and g values is not possible at this time because of the lack of sufficient information (such as optical absorption data) for determining the various crystal-field parameters. It is noteworthy, however, that our observations are quite consistent with susceptibilities calculated by Kambe *et al.*[9] within the lowest orbital triplet of Co^{2+} if

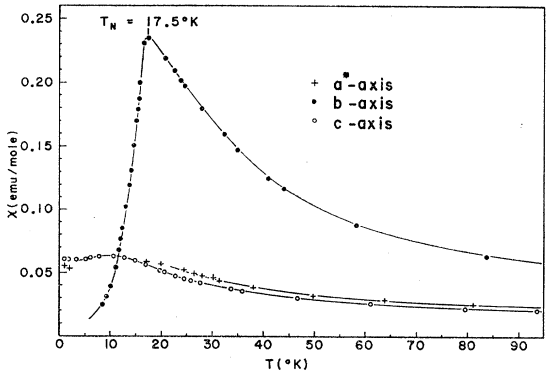

FIG. 4. Plot of single-crystal molar magnetic susceptibilities of $CoCl_2 \cdot 2H_2O$ as a function of temperature.

[8] A. Abragam and M. H. L. Pryce, Proc. Roy. Soc. (London) **A206**, 173 (1951).

[9] K. Kambe, S. Koide, and T. Usui, J. Phys. Soc. Japan **7**, 15 (1952).

[10] J. H. Van Vleck, *The Theory of Electric and Magnetic Susceptibilities* (Oxford University Press, New York, 1932), p. 181 ff.

we take $\eta \equiv 4\delta/3\lambda \simeq +5$, where δ is the tetragonal distortion parameter (i.e., the separation between the lowest levels in the absence of spin-orbit coupling) and $\lambda \simeq -180$ cm^{-1} is the spin-orbit coupling constant.

The small value of θ shows that the antiferromagnetic exchange forces acting on the Co^{2+} spins are compensated by ferromagnetic forces of essentially equal magnitude. Thus, ferromagnetic interactions must play an important role in determining the magnetic properties of $CoCl_2 \cdot 2H_2O$ despite its antiferromagnetic structure.

V. PROTON NUCLEAR MAGNETIC RESONANCE

The proton NMR in the paramagnetic state was observed in the liquid-hydrogen range; the onset of magnetic ordering was detected at 17.5 ± 0.1°K by the disappearance of the resonance on cooling through the transition.

A search for the zero-field proton NMR in the ordered state of $CoCl_2 \cdot 2H_2O$ yielded a single resonance.[11] The observed resonance, shown in Fig. 5, is a doublet with separation $\Delta\nu \simeq 50$ kc/sec, presumably due to dipolar spin-spin interactions between the two protons of the water molecule. (In the following discussion of the proton spectra all frequencies refer to the central frequency of the doublet.) The zero-field frequency, extrapolated to $T=0$°K, is $\nu_0(^1H) = 17.944 \pm 0.003$ Mc/sec corresponding to an internal field H_I at every proton site (due to the ordered Co^{2+} spins) of 4.214 kOe. Below 4°K the zero-field resonance exhibits a negligible temperature dependence; between 4 and 16°K, the observed frequencies accurately follow a $(\nu_0 - \nu) \propto T^{6.5}$ relation with an extrapolated zero-frequency temperature of 19.8°K. This behavior of the sublattice magnetization provides evidence for a large gap in the spin-wave spectrum and is qualitatively consistent with the large magnetic anisotropy inferred from the measured g values.

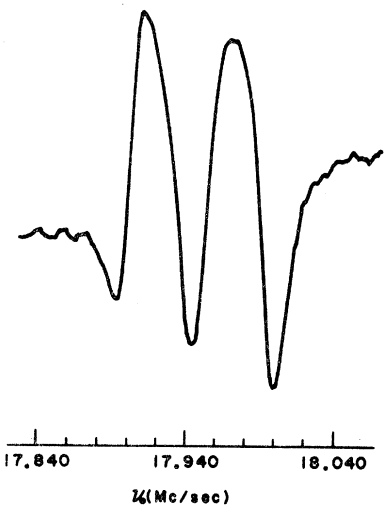

FIG. 5. Second derivative absorption spectrum of zero-field proton resonance in $CoCl_2 \cdot 2H_2O$ at 4°K.

[11] A. Narath, B. Morosin, and A. T. Fromhold, Jr., Bull. Am. Phys. Soc. 8, 359 (1963).

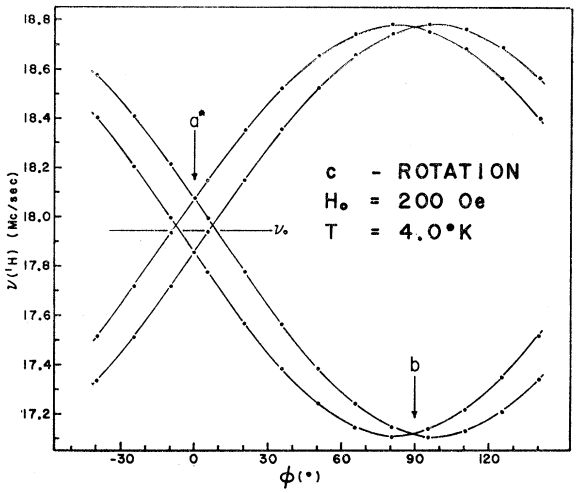

FIG. 6. Proton resonance diagram for rotation of $H_0 = 200$ Oe in a^*b plane at 4.0°K.

The eight protons in the chemical unit cell are all related by symmetry operations. (The two hydrogen atoms of each water molecule are related by the twofold axis, the two water molecules associated with a given cobalt ion are related by reflection symmetry, and the lattice centering operation provides the remaining equivalence.) The crystallographic equivalence of all proton positions, together with the existence of only a single internal field, require that the magnetic point group be identical to the crystallographic point group, except for the possible replacement of ordinary symmetry operations by antioperations. Hence, the Co^{2+} moments lie either along the b axis or in the ac plane. The magnetic susceptibility measurements, however, show unequivocally that the b axis is the preferred spin direction. We can conclude, therefore, that no appreciable canting occurs in the magnetic structure of $CoCl_2 \cdot 2H_2O$.

In order to determine the most probable spin arrangement, it is necessary to determine the direction of the internal field at the proton sites. This can be accomplished easily by observing the behavior of the nuclear resonance in weak external magnetic fields.[12] Since the spin direction has already been determined, it is only necessary to determine the absolute magnitudes of the internal-field components; hence, only a single field rotation is required.

If we assume that the directions of sublattice magnetization are unaffected by the external field, the resonance condition is

$$\omega/\gamma = H_T \equiv |(\mathbf{H}_0 + \mathbf{H}_I)|, \qquad (2)$$

where $\mathbf{H}_0$ is the external field and $\mathbf{H}_I$ is the internal field. In our experiments $\mathbf{H}_0$ was rotated in a plane normal to the c axis. We take ϕ to be the angle between $\mathbf{H}_0$ and

[12] N. J. Poulis and G. E. C. Hardeman, Physica 18, 201 (1952).

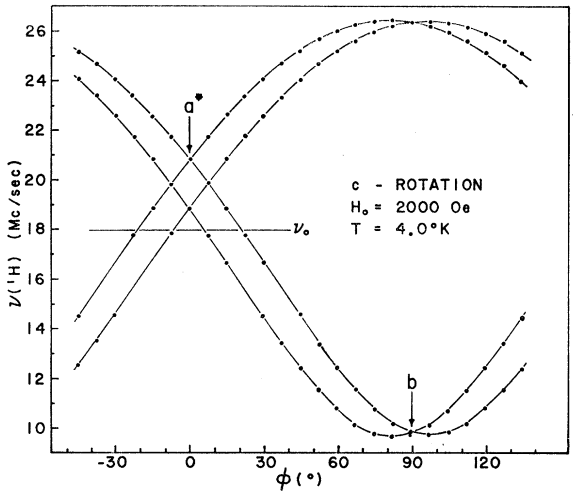

FIG. 7. Proton resonance diagram for rotation of $H_0=2000$ Oe in a^*b plane at 4.0°K.

the a^* axis, and choose a coordinate system in which the a^*, b, and c crystallographic axes lie along the x, y, z directions, respectively. The components of the net field are

$$H_T{}^x=H_0\cos\phi+H_I{}^x,$$
$$H_T{}^y=H_0\sin\phi+H_I{}^y,$$
$$H_T{}^z=H_I{}^z,$$

and the resonance condition becomes

$$\omega/\gamma=[H_0{}^2+H_I{}^2+2H_0H_I{}^{xy}]^{1/2}, \tag{3}$$

where

$$H_I{}^{xy}=H_I{}^x\cos\phi+H_I{}^y\sin\phi. \tag{4}$$

Since H_I is unusually large in $CoCl_2\cdot 2H_2O$, our rotation studies were carried out with $H_0<H_I$. Using this condition, the qualitative behavior of the resonance patterns can be obtained by expanding Eq. (3) in powers of H_0/H_I. The leading terms are given by

$$\frac{\omega}{\gamma}=H_I\left\{1+\frac{H_0{}^2}{2H_I{}^2}+H_I{}^{xy}\left[\frac{H_0}{H_I{}^2}-\frac{H_0{}^3}{2H_I{}^4}\right]-(H_I{}^{xy})^2\frac{H_0{}^2}{2H_I{}^4}+\cdots\right\}. \tag{5}$$

Since $H_I{}^{xy}$, the internal-field component in the direction of H_0, varies sinusoidally with ϕ, the resonance patterns are expected to be sinusoidal for sufficiently small values of H_0/H_I. The observed 4.0°K rotation patterns, shown in Fig. 6 for $H_0=200$ and in Fig. 7 for $H_0=2000$ Oe, follow these predictions and can be made to fit Eq. (3) exactly by a suitable choice of internal field parameters.

The observed rotation patterns have the 2π periodicity required of an antiferromagnetic structure, and are symmetric about the a^* and b axes. Only four distinct resonances are observed for a general orientation of the external field; the rotation patterns of the four signals

TABLE II. Comparison of calculated and observed proton local fields in antiferromagnetic $CoCl_2\cdot 2H_2O$, for spin ordering parallel to the b axis.

Space group	Spin structure J_L	J_T	Dipole field at ^1H position (kOe) $H_I{}^x$	$H_I{}^y$	$H_I{}^z$
I_c2/m	−	−	0.56	2.84	1.45
C_c2/m	−	+	1.28	2.91	0.62
P_C2/m	+	−	0.43	4.12	0.53
	Observed		0.546	4.134	0.607

are identical in shape and differ only in position along the ϕ axis. The two positions of maximum $H_I{}^{xy}$ occur at $\phi(\max)=(82.5,\ 97.5)\pm 0.1°$. The magnitude of $H_I{}^{xy}(\max)$ was calculated from the measured frequency at $\phi(\max)$, using the exact relation

$$H_I{}^{xy}(\max)=(H_T{}^2-H_I{}^2-H_0{}^2)/2H_0, \tag{6}$$

for values of H_0 ranging from 0.2–10 kOe. The average of our measurements gives

$$H_I{}^{xy}(\max)=4.170\pm 0.010\text{ kOe}.$$

The values of $H_I{}^x$, $H_I{}^y$, and $H_I{}^z$ follow immediately from H_I, $H_I{}^{xy}(\max)$, and $\phi(\max)$, and are given in the last line of Table II.

The internal field at the proton sites is the result of dipolar interactions with the Co^{2+} moments. The dipole fields can be calculated from

$$H_I{}^i=\sum_j B^{ij}, \tag{7}$$

$$B^{ij}=\int_0^\infty\left(\frac{3x^ix^j-\delta_{ij}r^2}{r^5}\right)\mu_j(\mathbf{r})d\tau, \tag{8}$$

where $H_I{}^i$ is the ith component of the dipole field and x^i, $x^j=x$, y, z are the components of the vector $\mathbf{r}$ which connects a given proton site to the volume element $d\tau$ having magnetic moment components $\mu_j(\mathbf{r})$. If we assume that the moment distribution around the Co^{2+} ions is spherical, the integral in Eq. (8) can be replaced by a sum over point dipoles. From a consideration of possible superexchange paths in $CoCl_2\cdot 2H_2O$, it follows that the most important exchange interactions should be the intrachain (J_L) coupling along the c axis and the nearest-neighbor interchain (J_T) coupling. We have computed the appropriate lattice dipole sums for the three magnetic structures shown in Fig. 8 which are consistent with the above arguments. The computations were carried out by direct summations over a sufficient number of lattice points within a spherical volume to assure an accuracy of $\pm 0.1\%$ in the calculated values.[13] The magnetic moment used in the calculation was $\mu_y(Co^{2+})=3.65\ \mu_B$ as determined from our susceptibility measurements. Since the limits of error in the x-ray determination of the hydrogen positions are quite

[13] B. Morosin and A. Narath, J. Chem. Phys. 40, 1958 (1964).

large, the geometry of the water molecule was adjusted to conform more closely to that found in other hydrated salts.[14] We chose O–H=0.97 Å and ∠H–O–H=108°, instead of the x-ray values of 0.85 Å and 102°, respectively. The hydrogen atoms were placed in the nearest-neighbor Cl–O–Cl plane as determined by the x-ray measurements. The components of $\mathbf{H}_I$ calculated in this way are compared in Table II with the experimental values. The agreement for a structure consisting of ferromagnetic chains with antiferromagnetic interchain couplings is seen to be quite good; the agreement for the two other structures, on the other hand, is very poor. We have examined the sensitivity of the fit to possible distortions in the moment distribution by calculating the contribution to $\mathbf{H}_I$ arising from any magnetic moment centered on the Cl^- ions. It was found that a 10% delocalization of the moment in the P_C2/m structure reduces the calculated values of $H_I{}^x$, $H_I{}^y$, and $H_I{}^z$ by 45, 9, and 30%, respectively. However, the conclusion that only the P_C2/m structure is capable of explaining both the magnitude of $\mathbf{H}_I$ and its small angular deviation from the b axis is not changed.

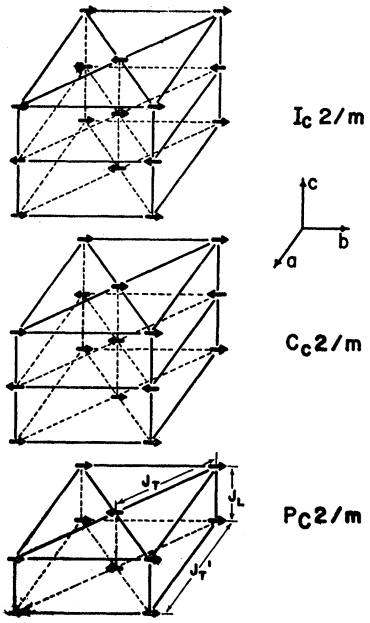

FIG. 8. Possible arrangements of Co^{2+} magnetic moments in the ordered structure of $CoCl_2 \cdot 2H_2O$ in zero external magnetic field.

VI. DISCUSSION

Our value of $T_N=17.5$°K agrees well with that determined recently by Shinoda *et al.*[15] from their observation of a λ-type specific heat anomaly at 17.20°K. This transition temperature is unusually high for a hydrated salt and results from the efficient packing which is inherent in the crystal structure of the dihydrated iron-group chlorides and bromides.

The intrachain exchange coupling proceeds through symmetric, ~90° Co–Cl–Co bridges. This linkage is identical to that responsible for the intralayer coupling in $CoCl_2$ ($T_N=25$°K[16]); in both cases this interaction is ferromagnetic. The antiferromagnetic nearest-neighbor interchain coupling in $CoCl_2 \cdot 2H_2O$ involves a Co–Cl–Cl–Co linkage (Cl–Cl=4.28 Å) similar to that responsible for the antiferromagnetic interlayer coupling in $CoCl_2$. In the case of $CoCl_2$, the ratio of the intralayer to interlayer exchange constants is ~13.[16] The small Curie-Weiss constant of $CoCl_2 \cdot 2H_2O$ can be understood by considering the relative number of neighbors which are coupled by the various interactions: The ferromagnetic interaction J_L couples each Co^{2+} spin to only two Co^{2+} neighbors; the antiferromagnetic interaction J_T, on the other hand, connects to twelve neighbors. Furthermore, it is likely that a third interaction J_T', involving Co–Cl–Cl–Co (Cl–Cl=3.81 Å) exchange paths along the a axis is important. The interaction couples to six neighbors, and is probably also antiferromagnetic. Thus, although the antiferromagnetic interactions are presumably much weaker than the ferromagnetic intrachain interaction, the fact that the former involve a much greater number of neighbors accounts for the small value of θ.

In the case of $CoCl_2 \cdot 6H_2O$, the ferromagnetic coupling J_L is entirely absent. The strongest coupling is antiferromagnetic and involves Co–Cl–Cl–Co bridges (Cl–Cl=4.07 Å)[17]; the ordering temperature is consequently quite low ($T_N=2.29$°K).[18]

That J_T' is not negligibly small is suggested by the observation of two discontinuities in the high-field magnetization ($H_0 \| b$) behavior of $CoCl_2 \cdot 2H_2O$.[19] Since J_T' couples *ferromagnetic* neighbors in the zero-field structure, it is possible that the first discontinuity involves a transition to a triangular spin arrangement. The determination of the magnitude of the various exchange constants and their anisotropies, on the basis of low- and high-field magnetization measurements, will be the subject of a future communication.

ACKNOWLEDGMENTS

The author wishes to express his gratitude to David C. Barham for his experimental assistance, to Dr. B. Morosin for many helpful discussions, and to E. J. Graeber for orienting our single-crystal specimens.

[14] S. W. Peterson and H. A. Levy, J. Chem. Phys. **26**, 220 (1957).
[15] T. Shinoda, H. Chihara, and S. Seki (to be published).
[16] M. E. Lines, Phys. Rev. **131**, 546 (1963); this work contains many of the earlier references.
[17] J. Mizuno, J. Phys. Soc. Japan **15**, 1412 (1960); R. D. Spence, P. Middents, Z. El Saffar, and R. Kleinberg, J. Appl. Phys. Suppl. **35**, 854 (1964).
[18] W. K. Robinson and S. A. Friedberg, Phys. Rev. **117**, 402 (1960).
[19] A. Narath and D. C. Barham, Bull. Am. Phys. Soc. **9**, 112 (1964).